Constraints on the Dark Matter Interpretation $n \to \chi + e^+ e^-$ of the Neutron Decay Anomaly with the PERKEO II Experiment

M. Klopf,[1] E. Jericha,[1] B. Märkisch,[2] H. Saul,[2,1] T. Soldner,[3] and H. Abele[1,*]

[1]*Atominstitut, Technische Universität Wien, Stadionallee 2, 1020 Wien, Austria*
[2]*Physik-Department ENE, Technische Universität München, James-Franck-Straße 1, 85748 Garching, Germany*
[3]*Institut Laue-Langevin, BP 156, 6, rue Jules Horowitz, 38042 Grenoble Cedex 9, France*

Discrepancies from in-beam- and in-bottle-type experiments measuring the neutron lifetime are on the 4σ standard deviation level. In a recent publication Fornal and Grinstein proposed that the puzzle could be solved if the neutron would decay on the one percent level via a dark decay mode, one possible branch being $n \to \chi + e^+ e^-$. With data from the PERKEO II experiment we set limits on the branching fraction and exclude a one percent contribution for 95% of the allowed mass range for the dark matter particle.

Neutron decay, as the prototype for nuclear beta decay, and its lifetime are needed to calculate most semileptonic weak interaction processes and used as input to search for new physics beyond the standard model of particle physics [1–4]. Measurements of the neutron lifetime fall into two categories [5]: in the storage method neutrons are confined in a material or magnetic bottle and after a given time the surviving neutrons are counted. In the beta decay method, the specific activity of an amount of neutrons (a section of a neutron beam, a neutron pulse, or stored neutrons) is measured by detecting one of the decay products, proton or electron. A review of neutron lifetime measurements can be found in Ref. [2]. The averaged results of both categories, 879.4(6) s and 888.0(2.0) s, deviate by 8.4 s from each other, corresponding to 4σ (all numbers from Ref. [6]).

Although this lifetime discrepancy may be related to underestimated systematics in experiments, there is a basic difference between the two categories: the storage method measures the inclusive lifetime, independent of the decay or disappearance channel, whereas the beta decay method detects the partial lifetime into a particular decay branch. Historically, Green and Thompson have used this argument to derive an upper limit on the decay into a hydrogen atom which would be missed by the beta decay method [5]; however, the expected branching fraction of 4×10^{-6} [7] is too small to explain the 8.4 s difference observed today. Greene and Geltenbort have speculated that the discrepancy might be caused by oscillations of neutrons into mirror

neutrons [8]. Recently, Fornal and Grinstein [9] have proposed different decay channels involving a dark matter particle. These branches would have been missed by the most precise beta decay method experiments which have detected decay protons [10].

Neutron stars have been used to severely constrain these branches [11,12] but some models evade these constraints [13]. Czarnecki *et al.* have derived a very general bound of $<0.27\%$ (95% C.L.) on exotic decay branches of the neutron, where they use their favored values of the neutron lifetime τ_n from the storage method and the axial coupling g_A from recent beta asymmetry measurements and assume that V_{ud} from superallowed beta decays and Cabibbo-Kobayashi-Maskawa (CKM) matrix unitarity are negligibly affected by exotic new physics. This means that not more than 2.4 s (with 95% C.L.) of the lifetime discrepancy might be explained by a dark decay. This constraint could be overcome by a smaller axial vector coupling constant g_A in the range $1.268 < g_A < 1.272$ [6], in contradiction to the most accurate measurements [14–16]. An extended analysis can be found in Ref. [17]. We note that the interpretation of the neutron decay anomaly is relevant for tests of the unitarity in the first row of the CKM matrix [18] with neutron decay. Recent reanalysis of the universal radiative correction Δ_R^V to neutron and superallowed nuclear beta decay raises tension with the CKM unitarity constraint based on superallowed $0^+ \to 0^+$ beta decays and Kaon decays [19].

Experimental constraints on the dark matter interpretation of the neutron decay anomaly have been set on two decay branches. A recent experiment at Los Alamos National Lab [20] excludes the proposed decay channel $n \to \chi + \gamma$ as sole explanation of the lifetime discrepancy with 97% C.L. via a direct search for a monoenergetic γ line. Another decay channel, $n \to \chi + e^+ e^-$, has been searched for by the UCNA collaboration [21]. For this decay channel, the sum of the kinetic energies of the

positron and electron $E_{e^+e^-} = E_{e^+} + E_{e^-}$ is restricted to the range of 0–644 keV, corresponding to a dark matter mass range of between 937.900 MeV and 938.543 MeV. The UCNA collaboration sets limits on this branching fraction of $< 10^{-4}$ (90% C.L.) in the energy range 100 keV $< E_{e^+e^-} < 644$ keV which excludes this channel as only explanation for the lifetime discrepancy at the 5σ level [21].

With this Letter, we set limits on the same decay channel $n \to \chi + e^+e^-$ from data taken by the PERKEO II instrument, which was installed at the PF1B cold neutron beam position [22,23] at the Institut Laue-Langevin (ILL). A drawing and a more detailed description of the PERKEO II spectrometer together with measurements of beta decay correlation coefficients can be found in Refs. [14,24–26]. For the investigation of a dark decay of the neutron into an e^+e^- pair, we reanalyze the data that were used to extract the beta asymmetry parameter A [14]. In that setup the spectrometer is configured for electron detection only. The electrons are transported from the decay volume towards either of the two detectors by a magnetic field of approximately 1 T. Details on the adiabatic transport of charged particles in magnetic fields can be found, e.g., in Ref. [27]. For the electron detection we used two plastic scintillators each read out by four fine mesh photomultiplier tubes (PMTs). The integrated pulse size of this detection system is largely proportional to the incident kinetic energy of a single electron or positron. During the measurements, the detector response function was determined and the detector stability checked regularly using four monoenergetic conversion electron sources. The detectors showed a nonlinearity at low energy, which was modeled for this search for a dark neutron decay mode using a quenching model developed by Birks [28]. This extends the analysis of Mund et al. [14]. The stopping power of electrons inside the scintillator material is calculated from ESTAR data [29]. The detector calibration, including the Birks nonlinearity parameter, was obtained by a fit to the electron spectra of each detector. The uncertainties in the nonlinearity relations of both detectors are taken into account for the analysis. The energy resolution does not play an important role for the present analysis, because a variation of 50% affects the limit on the dark matter e^+e^- branching ratio only on the 10^{-3} level.

About 8% of the electrons impinging on one of the detectors are scattered back from the detector and deposit only part of their energy in it. However, in the PERKEO II spectrometer such electrons will be guided along a magnetic field line to the other detector and will, a few nanoseconds later, deposit their energy there. For about half of the electrons, which are backscattered near the glancing angle, the fringe field of the magnet acts as a magnetic mirror and projects the electron back onto the same detector. So all electrons are confined by the magnetic field between the two detectors and can lose energy only to them. If, for each event, the total signal amplitudes from both detectors are added up, then the pure line spectrum is recovered. Details on the electron backscatter suppression can be found in Ref. [30].

The search for the proposed dark matter signal proceeded in the following way: Most of the conventional beta decay events were rejected by requiring that both detectors have triggered. For the remaining events, the spectrum of the total energy deposition was obtained by summing up the signals of both detectors. It is composed of conventional beta decay events with electron backscattering, background events that trigger both detectors, and of hypothetical e^+e^- events. Background events contribute with 2% to the spectrum and were measured regularly with the neutron beam closed and subtracted from the data. The e^+e^- pairs are monoenergetic and would create a characteristic peak on the backscattering spectrum, in the range from 0 to 644 keV depending on the mass of the hypothetical dark matter particle. Note that the selection cut excludes undetected backscattering events (see Refs. [31,32]) and e^+e^- pairs at low energy or going to the same detector. Positron annihilation gamma effects are small because of the low sensitivity of the thin (5 mm) plastic scintillators to 511 keV gammas and are taken into account in the analysis [33]. Tests with a ^{22}Na positron source were performed and the effects on the expected e^+e^- signal were simulated with GEANT4 [34].

The expected backscatter spectrum from conventional beta decay, which is the remaining background in the search for the hypothetical e^+e^- peak, is determined by simulations: Decay electrons are created with the angular and energy distribution from conventional neutron decay. For each electron, the impact angle on the detector is determined from the ratio of the magnetic field in the PERKEO II decay volume and at the detector.

Backscattering splits the kinetic energy of an electron in two parts deposited in the two detectors. It is simulated using GEANT4 [34] with the single Coulomb scattering model, which is appropriate for low energy backscattering as this option reproduces experimental data above a few tens of keV. In the few keV energy range some measurements find a different backscattering fraction [35]. We take this deviation as 1σ standard deviation error on our backscatter model. The magnetic mirror effect for backscattered electrons is taken into account in the simulations. For the energy splitting of e^+e^- events between both detectors, theoretical predictions from Ref. [36] are used. The resulting signals are obtained accounting for quenching in the scintillators, the statistical distribution of the photoelectron conversion of the PMTs (which is dominating the energy resolution), and additional broadening due to the noise of the charge to digital conversion.

The spectrum of the sum of the simulated signals still needs to be corrected for the trigger efficiencies of the two detectors. The experimental trigger efficiencies of both detectors are measured; for a signal in ADC channel C of detector 1, e.g., it is
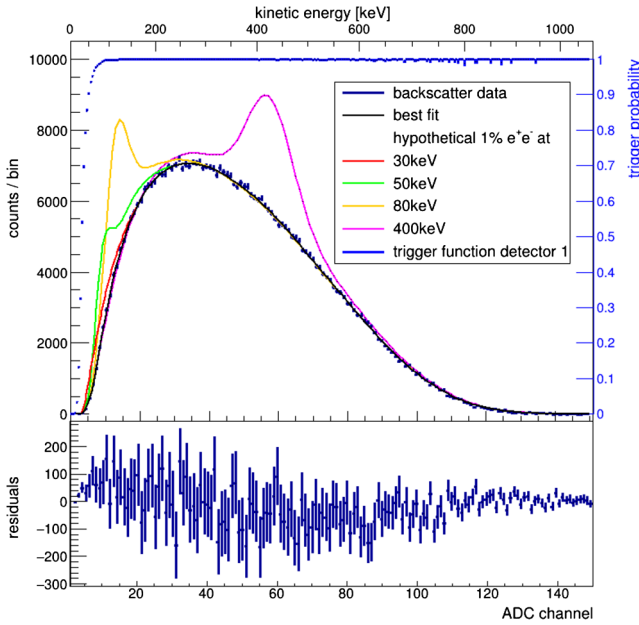
FIG. 1. Reanalysis of events of electrons backscattered from the PERKEO II detector system in a measurement of the beta correlation coefficient A and a search for an additional hypothetical dark matter e^+e^- signal. Shown is a fit with residuals to the summed coincidence spectrum together with a hypothetical $1\%e^+e^-$ branch at 30 keV, 50 keV, 80 keV, or 400 keV. The backscatter signal makes up approximately 4% of the total beta decay events, and is the sum of events registered in both detectors. We show the trigger probability for detector 1, too. The error bars show the statistical errors.

$$T_{\mathrm{exp},1}(C) = \frac{N_1(C, 1\,\&\,2)}{N_1(C, 2)}, \qquad (1)$$

where $N_1(C, 1\,\&\,2)$ is the number of events in detector 1 where both detectors have triggered and $N_1(C, 2)$ the number of events in detector 1 where detector 2 has triggered. For the hardware trigger condition of detector i at least two out of the four photomultipliers must have triggered.

The correction for the trigger efficiencies is obtained by applying, event by event, the trigger efficiency functions $T_{\mathrm{exp},i}$ to the simulated signals in the two detectors.

In Fig. 1 we show the experimental spectrum after background subtraction together with a fit using the results of the GEANT4 simulations. For illustration of the signature of the hypothetical e^+e^- peak, also shown is the expected shape of the spectrum for a 1% branching to χe^+e^- for e^+e^- total kinetic energies of 30 keV, 50 keV, 80 keV, and 400 keV. We scan the spectrum by shifting a hypothetical peak in steps of one channel of the analog to digital converter (ADC), which corresponds to approximately 6 keV, and performing a fit at each position. The height of the e^+e^- peak is the single free parameters of the fit. The phase space of e^+e^- pairs in the proposed dark decay has been computed in Ref. [36]. Under the assumption of a parity conserving dark decay, the probability that the
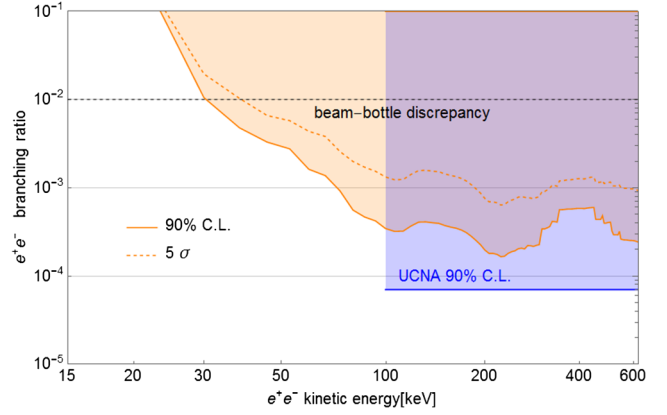
FIG. 2. Exclusion plot for a hypothetical e^+e^- dark matter branch in neutron beta decay for 90% C.L. and 5σ exclusion limits from a χ^2 analysis. The spectrum shown in Fig. 1 is scanned by shifting the energy of a potential e^+e^- peak in steps of one ADC channel, and performing a fit at each position. Free fitting parameter is the e^+e^- amplitude. On the 90% confidence limit a 1% contribution is excluded from 32 to 644 keV, which is the maximum energy according to Ref. [9]. The contributions of statistical and systematic errors are shown in Table I for selected ADC channels. For comparison we show approximate results of UCNA, extracted from Ref. [21].

electron and positron are emitted towards opposite detectors varies between 47.8% and 50%, depending on the mass of the dark matter particle. As only these events can pass our selection cut, we assume the most conservative case for the e^+e^- emission of 47.8% in the exclusion analysis.

In Fig. 2 we show an exclusion plot for a hypothetical χe^+e^- branching fraction at 90% C.L., which corresponds to a one sided 1.3σ cut above the best fit value for the dark matter branching ratio. In regions, where the fit to the amplitude of the dark matter signal has a negative outcome, we renormalize the tail probabilities in the positive range and take a 90% cut. We also tested the significance of observing a local excess of events, i.e., a dark matter signal somewhere in a possible mass range if we take into account the probability of observing such an excess anywhere in the range. We quantify this "look-elsewhere effect" by obtaining 10^7 Monte Carlo simulations of backscatter only

TABLE I. One sigma standard deviation error budget for the fit for a hypothetical e^+e^- dark matter branch shown in Fig. 2 at selected channels 5, 10, 50, 100. The backscatter model error includes the GEANT4 uncertainty in predicting the backscattering coefficient of electrons as a function of energy.

ADC channel	Statistical error	Calibration error	Backscatter model error
5	3.1×10^{-4}	4.09×10^{-4}	8.92×10^{-4}
10	1.50×10^{-4}	1.40×10^{-4}	5.98×10^{-4}
50	9.28×10^{-5}	9.11×10^{-5}	9.28×10^{-5}
100	4.12×10^{-5}	1.37×10^{-4}	3.47×10^{-5}

data, and for each channel the largest fluctuation that resembles a signal. Details on the look-elsewhere effect can be found, e.g., in Ref. [37]. The proposed 1% contribution to neutron beta decay [9] can be excluded with 90% C.L. between 32 keV and 664 keV and better than 5 sigma standard deviation for energies between 37.5 keV and 664 keV. This corresponds to 95%, and 94%, respectively, of the allowed mass range for the dark matter particle. In general we can derive limits for higher energies, which are, however, excluded by Ref. [9].

---

*Corresponding author.
abele@ati.ac.at

[1] D. Dubbers and M. G. Schmidt, Rev. Mod. Phys. **83,** 1111 (2011).

[2] F. E. Wietfeldt and G. L. Greene, Rev. Mod. Phys. **83,** 1173 (2011).

[3] H. Abele, Prog. Part. Nucl. Phys. **60,** 1 (2008).

[4] M. González-Alonso, O. Naviliat-Cuncic, and N. Severijns, Prog. Part. Nucl. Phys. **104,** 165 (2019).

[5] K. Green and D. Thompson, J. Phys. G **16,** L75 (1990).

[6] A. Czarnecki, W. J. Marciano, and A. Sirlin, Phys. Rev. Lett. **120,** 202002 (2018).

[7] L. L. Nemenov, Sov. J. Nucl. Phys. **31,** 115 (1980).

[8] G. L. Greene and P. Geltenbort, Sci. Am. **314,** 36 (2016).

[9] B. Fornal and B. Grinstein, Phys. Rev. Lett. **120,** 191801 (2018).

[10] A. T. Yue, M. S. Dewey, D. M. Gilliam, G. L. Greene, A. B. Laptev, J. S. Nico, W. M. Snow, and F. E. Wietfeldt, Phys. Rev. Lett. **111,** 222501 (2013).

[11] G. Baym, D. H. Beck, P. Geltenbort, and J. Shelton, Phys. Rev. Lett. **121,** 061801 (2018).

[12] D. McKeen, A. E. Nelson, S. Reddy, and D. Zhou, Phys. Rev. Lett. **121,** 061802 (2018).

[13] J. M. Cline and J. M. Cornell, J. High Energy Phys. 07 (2018) 81.

[14] D. Mund, B. Märkisch, M. Deissenroth, J. Krempel, M. Schumann, H. Abele, A. Petoukhov, and T. Soldner, Phys. Rev. Lett. **110,** 172502 (2013).

[15] M. P. Mendenhall et al. (UCNA Collaboration), Phys. Rev. C **87,** 032501(R) (2013).

[16] B. Märkisch, H. Mest, H. Saul, X. Wang, H. Abele, D. Dubbers, M. Klopf, A. Petoukhov, C. Roick, T. Soldner, and D. Werder, arXiv:1812.04666.

[17] D. Dubbers, H. Saul, B. Märkisch, T. Soldner, and H. Abele, Phys. Lett. B **791,** 6 (2019).

[18] H. Abele, B. Barberio, D. Dubbers, F. Glück, J. Hardy, W. Marciano, A. Serebrov, and N. Severijns, Eur. Phys. J. C **33,** 1 (2004).

[19] C.-Y. Seng, M. Gorchtein, H. H. Patel, and M. J. Ramsey-Musolf, Phys. Rev. Lett. **121,** 241804 (2018).

[20] Z. Tang et al., Phys. Rev. Lett. **121,** 022505 (2018).

[21] X. Sun et al. (UCNA Collaboration), Phys. Rev. C **97,** 052501 (2018).

[22] H. Häse, A. Knöpfler, K. Fiederer, U. Schmidt, D. Dubbers, and W. Kaiser, Nucl. Instrum. Methods Phys. Res., Sect. A **485,** 453 (2002).

[23] H. Abele, D. Dubbers, H. Häse, M. Klein, A. Knöpfler, M. Kreuz, T. Lauer, B. Märkisch, D. Mund, V. Nesvizhevsky, A. Petoukhov, C. Schmidt, M. Schumann, and T. Soldner, Nucl. Instrum. Methods Phys. Res., Sect. A **562,** 407 (2006).

[24] M. Schumann, M. Kreuz, M. Deissenroth, F. Glück, J. Krempel, B. Märkisch, D. Mund, A. Petoukhov, T. Soldner, and H. Abele, Phys. Rev. Lett. **100,** 151801 (2008).

[25] M. Schumann, T. Soldner, M. Deissenroth, F. Glück, J. Krempel, M. Kreuz, B. Märkisch, D. Mund, A. Petoukhov, and H. Abele, Phys. Rev. Lett. **99,** 191803 (2007).

[26] J. Reich, H. Abele, M. Hoffmann, S. Baeßler, P. Bülow, D. Dubbers, V. Nesvizhevsky, U. Peschke, and O. Zimmer, Nucl. Instrum. Methods Phys. Res., Sect. A **440,** 535 (2000).

[27] D. Dubbers, L. Raffelt, B. Märkisch, F. Friedl, and H. Abele, Nucl. Instrum. Methods Phys. Res., Sect. A **763,** 112 (2014).

[28] J. D. Birks, Proc. Phys. Soc. London Sect. A **64,** 874 (1951).

[29] M. J. Berger, J. S. Coursey, M. A. Zucker, and J. Chang, ESTAR, PSTAR, and ASTAR: Computer Programs for Calculating Stopping-Power and Range Tables for Electrons, Protons, and Helium Ions (National Institute of Standards and Technology, Gaithersburg, MD, 2005), http://physics.nist.gov/Star.

[30] H. Abele, G. Helm, U. Kania, C. Schmidt, J. Last, and D. Dubbers, Phys. Lett. B **316,** 26 (1993).

[31] M. Schumann and H. Abele, Nucl. Instrum. Methods A **585,** 88 (2008).

[32] C. Roick, H. Saul, H. Abele, and B. Märkisch, in Proceedings of International Workshop on Particle Physics at Neutron Sources (to be published).

[33] M. Klopf, E. Jericha, B. Märkisch, H. Saul, T. Soldner, and H. Abele, in Proceedings of International Workshop on Particle Physics at Neutron Sources (to be published).

[34] S. Agostinelli et al., Nucl. Instrum. Methods Phys. Res., Sect. A **506,** 250 (2003).

[35] S. H. Kim, M. G. Pia, T. Basaglia, M. C. Han, G. Hoff, C. H. Kim, and P. Saracco, IEEE Trans. Nucl. Sci. **62,** 451 (2015).

[36] A. N. Ivanov, R. Höllwieser, N. I. Troitskaya, M. Wellenzohn, and Y. A. Berdnikov, arXiv:1806.10107.

[37] E. Gross and O. Vitells, Eur. Phys. J. C **70,** 525 (2010).